Research Article

Modelling of Gassing for VRLA OPzV (gel) Battery at 25°C

Jibran Hayat* and Nisai H. Fuengwarodsakul
The Sirindhorn International Thai-German Graduate School of Engineering, King Mongkut's University of Technology North Bangkok, Bangkok, Thailand

Jeanette Muenderlein and Timo Ruewald
Institute of Power Electronics and Electrical Drives (ISEA), RWTH Aachen University, Aachen, Germany

* Corresponding author. E-mail: jibranhayat@gmail.com   DOI: 10.14416/j.asep.2019.02.001

Abstract
In order to increase the performance of the Energy Management System (EMS) for the M5BAT (Modular Multi-Megawatt Multi-Technology Middle Voltage Battery Storage System), with a size of 5 MW and to take full economic advantage of the various lead-acid batteries, battery models are implemented. Based on such models, a technology specific and favorable operation can be assured. For improving the model an experimental study of gassing has been conducted on the Sonnenschein A602 OPzV VRLA (gel) battery. Single electrode potentials have been observed and evaluated at different current rates at a regulated temperature of 25°C. Parameters such as the symmetry factor and current exchange density have been obtained from the measured data. Matlab/Simulink has been used to model the process of gassing using Tafel´s equations.

Keywords: Gassing, Overpotential, Current exchange density, Symmetry factor, Gassing equilibrium potential

1 Introduction

The electric power grid does not possess the capability to store energy unlike other energy supply networks such as a gas grid. Therefore, in an electric grid the feed-in power (generation) must be equal to the power consumed (load) so that it is stable at all times. Within a time range of seconds up to a few-hours, Battery Energy Storage System(BESS) can be a well-fitting option for the frequency stabilization of the middle voltage grid. Furthermore, the trading on the German exchange market of Frequency Control Reserve (FCR) represents the most profitable option, at the moment.

Using Battery Energy Storage System (BESS) as FCR supply initially started in the 1980s [1]. The utility BEWAG in Berlin operated a BESS of 17 MW/ 14 MWh, for frequency regulation based on lead-acid batteries successfully between 1986 and 1993 [2].

One of the biggest challenges for any BESS as FCR is to reduce operational costs to increase profitability. Historically, BESS for frequency regulation has been limited to a few applications primarily due to limited service life and high battery costs [3]. However, with significant advancement in lead-acid cell technologies in terms of cyclic stability, improved performance and longevity the overall situation for BESS to be used a FCR has improved [4].

To find out how profitable a BESS system can operate in the FCR market with different cell technologies, the M5BAT project was established. M5BAT (5 MW) BESS consists of different battery strings i.e. Lead-acid (OCSM), VRLA gel (OPzV) and three Lithium-ion cell technologies (Lithium-Manganese-Oxide, Lithium-Iron-Phosphate, Lithium-Titanite-Oxide). Out of these

battery strings, VRLA (OPzV) contributes 1 MW to BESS. BESS is operating in Aachen since September 2016 [5]. One of the project aims is to develop a sophisticated Energy Management System (EMS) for cost-effective operation of BESS. The EMS is based on battery models, which include the technology specific characteristics of each battery string. In the context of Model-Based Energy Management System, it is very vital to understand and stimulate the cell-behavior in detail.

In this research work, the focus is laid on the investigation of gassing behavior of Sonnenschein A602 OPzV Valve Regulated Lead Acid battery (VRLA) with gelled electrolyte, which is one of the 5 different cell technologies used in the M5BAT. The main objective of this research is to develop sub-models of the gassing processes (see section 3) in the VRLA (OPzV) battery, which will then be integrated with an overall model of VRLA (OPzV) battery for simulation of its dynamic operations. To ensure a high accuracy, the parameterization of the gassing model is done by gassing measurements of VRLA (OPzV) battery.

2 General Characteristics and Design of VRLA Battery

One typical characteristic of lead-acid batteries is that when fully charged the additional current goes into gassing reactions. At the positive electrode, oxygen is produced while the negative electrode experiences the evolution of hydrogen. This phenomenon causes substantial loss of water over time, therefore flooded batteries must be refilled with water from time to time requiring regular maintenance. This drawback of flooded cell technology is overcome by so-called Valve Regulated Lead Acid Batteries (VRLA) [6].

The VRLA is different from flooded-cell technology in terms of electrolyte and internal oxygen reduction cycle (see Figure 1). In VRLA batteries there is starved electrolyte Absorbed in Glass Mat (AGM) or gelled electrolyte. In most of VRLA battery design, the capacity of the cell is limited by the quantity of Positive Active Mass (PAM). The combination of starved electrolyte and a large quantity of Negative Active Mass (NAM) enables oxygen recombination at negative electrode during overcharge of the battery [7]. The valves release the internal gasses when the
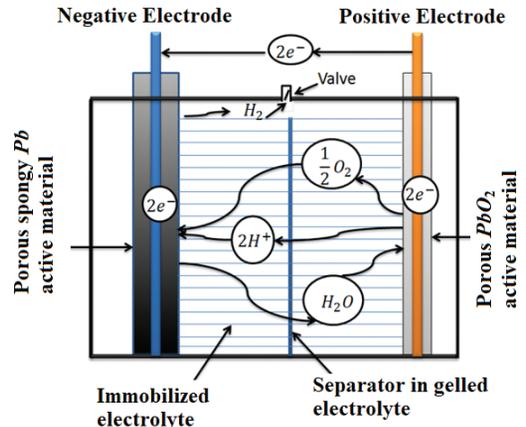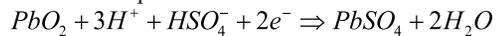

Figure 1: Gassing and oxygen recombination process in VRLA battery.

pressure reaches its threshold limit. The design of vent pressure is determined by the manufacturer and most importantly it depends on case shape and material [8].
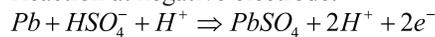
2.1 Working principle

VRLA battery design differs from flooded lead-acid battery yet the chemistry is same in both cases. The overall reaction holds to "double sulfate reaction" [7]:
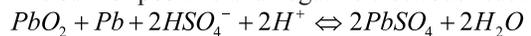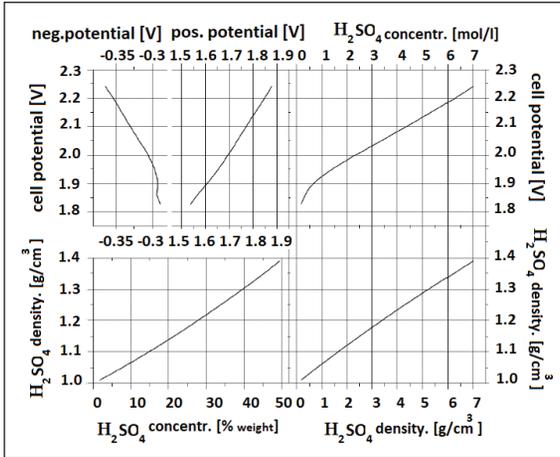
Reaction at positive electrode:
$$PbO_2 + 3H^+ + HSO_4^- + 2e^- \Rightarrow PbSO_4 + 2H_2O$$

Reaction at negative electrode:
$$Pb + HSO_4^- + H^+ \Rightarrow PbSO_4 + 2H^+ + 2e^-$$

The sum of positive and negative electrode reaction :
$$PbO_2 + Pb + 2HSO_4^- + 2H^+ \Leftrightarrow 2PbSO_4 + 2H_2O$$

The electrolyte in lead-acid battery plays a very important role because it provides the ionic conductivity and it serves as an electrochemical reactant. Consequently, the concentration of electrolyte increases almost linearly during charging and decreases while discharging.

There are numerous denotations of the concentration of electrolyte, and the most common of which is through "acid density. In Figure 2 the corresponding potentials (positive electrode, negative electrode and terminal voltage) are illustrated along "acid density" in relation to mass percentage (%weight) and molarity (mol/L) [9].

Figure 2: Electrolyte concentration expressed as %weight, corresponding cell potentials and electrode potentials at equilibrium state [9].

2.2 Reaction Kinetics

To drive the electrode reactions at a certain required current rate, additional energy is needed. This additional energy is known as an electrode overpotential. The overpotential η is a measure of deviation of the actual electrode potentials U^+ and U^- from their respective electrochemical equilibrium potentials U_O^+ and U_O^- [see Equations (1) and (2)]

Positive electrode overpotential

$$h^+ = U^+ - U_O^+ \tag{1}$$

Negative electrode overpotential

$$h^- = U^- - U_O^- \tag{2}$$

The measurable overpotential is caused by various effects listed below:
- Activation overpotential η_{act}
- Concentration overpotential η_{con}
- Crystallization overpotential η_{cry}
- Resistive (ohmic) overpotential η_{ohm}

The polarity signs (+ and −) are omitted due to the fact that it is true for both electrodes [Equations (3) and (4)].

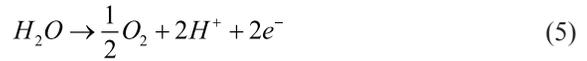$$\eta = \eta_{act} + \eta_{con} + \eta_{cry} + \eta_{ohm} \tag{3}$$

$$\eta = U - U_O \tag{4}$$

As reported in literature the experimentally observed typical gradient for overpotential per current decade of gassing current is –120 mV for the negative electrode and 80 mV for the positive electrode respectively. The low gassing rate results in "quasi-stability" of the lead-acid battery systems [10].

2.3 Gassing and internal oxygen cycle in VRLA

In lead-acid batteries apart from the main reactions (see section 2.1), gas evolution is always present on both electrodes [see Equations (5) and (6)] [7]. Hydrogen evolves at the negative electrode and oxygen at the positive electrode. Overall gassing reaction is illustrated by Equation (7).

Oxygen evolution at the positive electrode

$$H_2O \rightarrow \frac{1}{2}O_2 + 2H^+ + 2e^- \tag{5}$$

Hydrogen evolution at the negative electrode

$$2H^+ + 2e^- \rightarrow H_2 \tag{6}$$
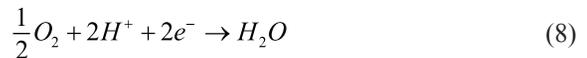
The overall gassing reaction
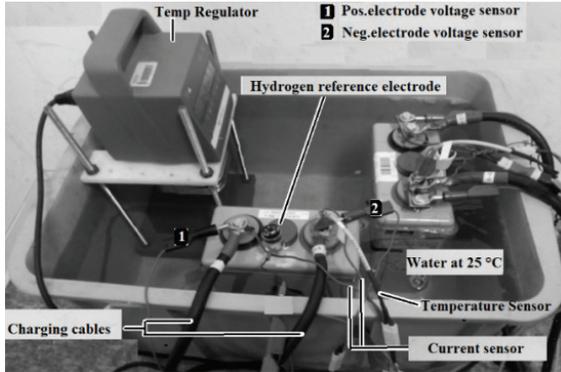
$$H_2O \rightarrow H_2 + \frac{1}{2}O_2 \tag{7}$$

Contrary to flooded type batteries, in VRLA the overcharging and float-charging situation is characterized by the internal oxygen-cycle. The narrow cracks in starved electrolyte permit the flow of oxygen generated at positive electrode to the negative electrode, where it is reduced to water [see Equation (8)].

Recombination process at negative electrode

$$\frac{1}{2}O_2 + 2H^+ + 2e^- \rightarrow H_2O \tag{8}$$

3 Modelling Approach for Gassing in VRLA Battery

Reactions at the positive and negative electrode for gassing current density i_gas can be approximated by the Tafel Equations (9) and (10) [11].

Figure 3: Gassing test setup at 25 degrees Celsius, ISEA-RWTH Aachen, Germany 2017.

Gassing current density at the Positive electrode

$$i^+_{gas} = i^+_{o,gas} \times e\left[\frac{n \times \eta^+_{gas} \times \alpha^+_{gas}}{U_T}\right] \quad (9)$$

Gassing current density at the negative electrode

$$i^-_{gas} = i^-_{o,gas} \times e\left[\frac{-n \times \eta^-_{gas}(1 - \alpha^-_{gas})}{U_T}\right] \quad (10)$$

- Current exchange density $\rightarrow i_{o,gas}$
- Number of transferred elementary charges (valency) $\rightarrow n = 2$
- Temperature Voltage

$$\rightarrow U_T = \frac{R \times T}{F} = 26 \text{ mV}$$

T = 298 K
Gas constant(R) = 8.314 $JK^{-1}mol^{-1}$
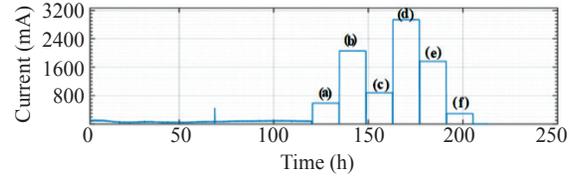Faradaic constant(F) = 96485.3 C mol^{-1}
- Symmetric coefficient $\rightarrow \alpha$

4 Experimental Setup for Measurement of Gassing in VRLA Battery

Sonnenschein A602 OPzV battery with a nominal capacity of 294 Ah has been used to perform the experiment. Single electrode potentials have been observed and evaluated at different current rates at a regulated temperature of 25°C (see Figure 3).

For measuring the potential of the negative and the positive electrode a hydrogen reference electrode was used. The hydrogen reference electrode was

Figure 4: overcharging constant current steps (phases) of gasing test.

positioned at top of the cell between the two electrodes (see Figure 3). Then the hole was sealed properly to make it air tight so that no oxygen from atmosphere could enter the battery and affects the behavior of the VRLA battery.

4.1 Gassing test with high overcharging currents

The measurement started with a constant voltage phase of 2.4 V for 5 days (120 h) in order to achieve a fully charged state of the cell [100% state of charge (SOC)]. Only then it can be ensured that the further charging current exclusively goes in the gassing reactions.
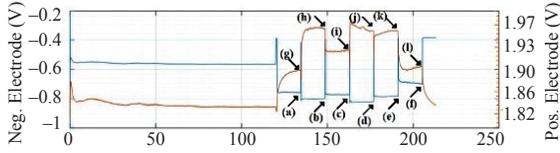
Table 1: overcharging constant current step values of the gassing test from Figure 3

Overcharging Step	Overcharging Step Values (14 h each)
(a)	500 (mA)
(b)	2000 (mA)
(c)	800 (mA)
(d)	3000 (mA)
(e)	800 (mA)
(f)	300 (mA)

Each of the constant current step (phase) took 14 h. Figure 4 shows the profile of the current applied to the battery and Table 1 refers to the exact values of each constant current step (phase) from the Figure 4. In total, both constant voltage and constant current phases took 8.5 days (204 h) to complete the test.

Table 2: Values of measured positive and negative electrode potentials from Figure 5

Measured U_- (V)		Measured U_+ (V)	
(a)	−0.7580	(g)	1.8981
(b)	−0.8007	(h)	1.971
(c)	−0.7722	(i)	1.9326
(d)	−0.8281	(j)	1.9658
(e)	−0.7841	(k)	1.9658
(f)	−0.6967	(l)	1.9041

Figure 5: Measured potentials of positive and negative electrode.

Measured electrode potentials point are taken at the end of each corresponding constant current steps (phases) see Figure 4. The resulting behavior of the battery during overcharging steps (phases) for the positive and the negative electrode potentials with reference to hydrogen electrode are shown in Figure 5 and Table 2 refers to values of electrode potentials from Figure 5. The negative electrode potentials depicts a stable and expected behavior for different current rates. The positive electrode potentials shows polarization of voltages for all corresponding constant currents except the corresponding voltage (see point (j) Figure 5) for the fourth constant current step (see point (d) Figure 3). There could be two reasons, first because of the instability caused by hydrogen reference electrode and second the positive electrode was not charged to its full capacity. Since the battery was charged to 100% SOC for 5 days, the decline in the electrode potential during 3000 mA constant current phase is probably caused by momentary instability of the hydrogen electrode and led to decline of voltage.

For gassing measurements, the typical change in overpotential per current decade for the positive electrode is reported as 80 mV and –120 mV for the negative electrode [11].

In Figure 6, the y-axes represents semilogarithmic (base 10) current in mA/100Ah and the x-axes represents overpotential/overvoltage in mV. The overpotential is calculated from the following equation.

Overpotential/Overvoltage for positive electrode [Equations (11) and (12)]:

$$\eta_+ = U_+^O - U_+ \qquad (11)$$

Overpotential/Overvoltage for negative electrode

$$\eta_- = U_-^O - U_- \qquad (12)$$

U_+ is the measured positive electrode potential with respect to hydrogen reference electrode while U_O^+

is equilibrium potential (O_2 potential). Similarly, U_- is the measured negative electrode potential with respect to hydrogen reference electrode and U_O^- is equilibrium potential (H_2 potential). Under standard conditions U_O^+ accounts for 1.229 V and U_O^- for 0 V against Standard Hydrogen Electrode (SHE) [7]. Equilibrium potential depends upon the acid density and thus upon the stage of charge. The respective equilibrium potentials were calculated by applying Nernst Equation [7] (see Table 3). Equilibrium potentials are taken for an acid density of 1.3 $\frac{g}{cm^3}$, since the battery is charged to 100% SOC. This value of acid density is in the expected range (see Table 4).

Table 3: Calculated values for gassing equilibrium potentials depending upon acid density

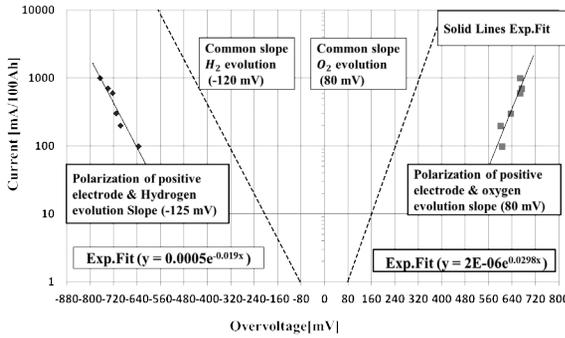| Acid density ($\frac{g}{cm^3}$)	H_2 Potential (V)	O_2 Potential (V)
1	−0.081259	1.14774
1.01	−0.041101	1.18789
1.02	−0.026050	1.20294
1.03	−0.016565	1.21243
1.04	−0.009610	1.21938
1.06	0.000449	1.22944
1.08	0.007745	1.23674
1.1	0.013489	1.24248
1.14	0.022292	1.25129
1.18	0.028985	1.25798
1.22	0.034411	1.26341
1.26	0.034411	1.26798
1.3	0.042959	1.29765

Table 4: Typical acid density values VRLA and SLI lead-acid batteries at 100% SOC [12]

Battery Type	Unit	Densities at 100%SOC
Flooded SLI	g/cm³ or Kg/l	1.28
VRLA/AGM SLI	g/cm³ or Kg/l	1.29–1.33

From Figure 6, the exponential fit [see Equation (13)] of the positive electrode corresponds with the Tafel´s equation [see Equation 8)].

Exponential fit of the positive electrode:

$$i_{gas}^+ = 2^{-06} e^{(0.0298 \times \eta_{gas}^+)} \qquad (13)$$

Figure 6: Evaluation of gassing test for the positive and the negative electrode.

Figure 7: Matlab/Simulink gassing block diagram.

Symmetry factor (alpha):

$$\frac{n \times \alpha^+_{gas}}{U_T} = 0.0298 mV \rightarrow \alpha^+_{gas} = 0.3874$$

Current exchange density:

$$i^+_{gas} = 2^{-06}$$

Exponential fit of the negative electrode:

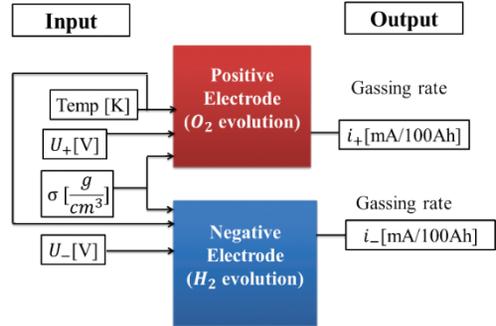$$i^-_{gas} = 5^{-04} e^{(-0.019 \times \eta^-_{gas})} \tag{14}$$

Symmetry factor (alpha):

$$\frac{-n(1 - \alpha^-_{gas})}{U_T} = -0.019 mV \rightarrow \alpha^-_{gas} = 0.7530$$
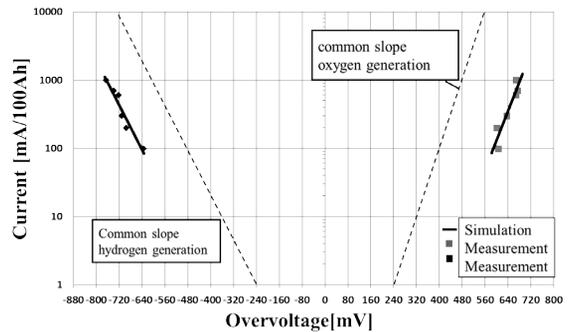
Current exchange density:

$$i^-_{gas} = 5^{-04}$$

Both the positive and negative electrodes show nearly an exponential behavior for the gassing test. From the Figure 6, we can see an overpotential per decade change of –125 mV for the negative electrode (left-hand side) and 80 mV for the positive electrode (right-hand side). Solid lines are an exponential fit of the measurement data. Dashed lines represent the common slope for oxygen generation at the positive electrode and hydrogen generation at the negative electrode as reported in literature [11], [12]. From evaluation of the gassing test, it can be clearly seen that the results for Sonnenschein A602 (OPzV) VRLA battery are in line with the results from literature.

Figure 8: Simulation results of simplified interface of gassing model.

Parametrization of gassing model is done with the help of exponential fit equations which corresponds to Tafel´s equations of gassing currents.

5 Gassing Model

The positive gassing block and the negative gassing block were modelled in Matlab/Simulink by implementing Tafel´s equations [see Equtions (9) and 10)]. The block diagram (as shown in Figure 7) indicates the inputs it requires to calculate gassing rates for the positive and the negative electrode.

To evaluate the gassing modelling, measured values of the electrode potentials (U_+ and U_-) were input to the positive and negative gassing blocks (see Figure 7). The validation of simplified interface of gassing model is based on the parametrization of model with real experimental data and the simulation results can be well fitted with Tafel equations (see Figure 8 and Table 5).

Table 5: Parameters for gassing model

Parameter	Origin	Value/Remarks
Temperature of battery (K)	Simulation (constant)	298.15 K
Acid density (σ)	Literature	1.3 g/cm^3
Positive electrode (U_+)	Experimental values	1.9658 V (e.g.)
Negative electrode (U_-)	Experimental values	–0.8007 V (e.g.)
Symmetry factor (α_{gas}^+)	Exponential fitting	0.3874
Symmetry factor (α_{gas}^-)	Exponential fitting	0.7530
Current exchange density ($i_{O,gas}^+$)	Exponential fitting	2^{-06}
Current exchange density ($i_{O,gas}^-$)	Exponential fitting	5^{-04}

6 Conclusions

An experimental study of gassing has been conducted on Sonnenschein A602 OPzV (gel) battery for modelling of gassing and parametrization of a model for EMS. Single electrode potentials have been monitored and evaluated at different current rates at a regulated temperature of 25°C. The overpotential per decade change for the negative electrode is –125 mV and 80 mV for the positive electrode. Parameters such as symmetry factor and current exchange density have been obtained from experimental data.

The Matlab/Simulink blocks have been used to realize the process of overcharging by using Tafel´s equations for the gassing currents and it is basically a simplified interface for gassing behaviour of battery. The model depicts the oxygen evolution at the positive electrode as exponential behaviour (see Figure 8: right-hand side) and for the negative electrode hydrogen evolution as exponential behaviour as well (see Figure 8: left-hand side). The simulation results of simplified interface of gassing model are in accordance with experimental data (see Figure 6) and can be well fitted with Tafel equations.

References

[1] H. J. Kunisch, K. G. Kramer, and H. Dominik, "Battery energy storage another option for load-frequency-control and instantaneous reserve," *IEEE Transactions on Energy Conversion*, vol. EC-1, no. 3, pp. 41–46, Sep. 1986.

[2] J. Fleer and P. Stenzel, "Impact analysis of different operation strategies for battery energy storage systems providing primary control reserve," *Journal of Energy Storage*, vol. 8, pp. 320–338, Nov. 2016.

[3] D. H. Doughty, P. C. Butler, A. A. Akhil, N. H. Clark, and J. D. Boyes, "Batteries for large-scale stationary electrical energy storage," *The Electrochemical Society Interface*, vol. 19, no. 3, pp. 49–53, 2010.

[4] S. S. Misra, S. L. Mraz, J. D. Dillon, and D. B. Swanson, "VRLA Battery with AGM-gel hybrid for superior performance" in *Proceedings of The 25th International Telecommunications Energy Conference*, 2003, pp. 378–382.

[5] M5BAT. (2016, Sep.). M5BAT: A Unique Hybrid Battery Storage System. M5BAT. Aachen, Germany [Online]. Available: http://m5bat.de/en-gb/

[6] D. Berndt, "Valve-regulated Lead-acid batteries," *Journal of Power Sources*, vol. 100, pp. 29–46, 2001.

[7] D. Berndt, *Maintenance-Free Batteries: Based on Aqueous Electrolyte Lead-Acid, Nickel/Cadmium, Nickel/Hydride; A handbook of battery technology*, 3rd ed., Taunton, UK: Research Studies Press, 2003.

[8] D. Linden and T. B. Reddy, *Handbook of Batteries,* 3rd ed., New York: McGraw-Hill, 2002.

[9] D. U. Sauer, "Optimierung des einsatzes von blei-säure-akkumulatoren n photovoltaik-hybrid-systemen unter spezieller berüksichtigung der batteriealterung," Ph.D. dissertation, Dessertation, University of Ulm, Germany, 2003.

[10] A. Hammouche, M. Thele, and D. U. Sauer, "Analysis of gassing processes in a VRLA/spiral wound battery," *Journal of Power Sources*, vol. 158, pp. 987–990, 2006.

[11] M. Thele, *A Contribution to the Modelling of the Charge Acceptance of Lead-acid Batteries: Using Frequency and Time Domain Based Concepts*. Aachen, Germany: Shaker Verlag Gmbh, 2008.

[12] H. Bode, *Lead-acid Batteries*. New York: Wiley, 1977.